We are IntechOpen, the world's leading publisher of Open Access books Built by scientists, for scientists

4,800
Open access books available

122,000
International authors and editors

135M
Downloads

Our authors are among the

154
Countries delivered to

TOP 1%
most cited scientists

12.2%
Contributors from top 500 universities

CLARIVATE ANALYTICS BOOK CITATION INDEX INDEXED

WEB OF SCIENCE™

Selection of our books indexed in the Book Citation Index in Web of Science™ Core Collection (BKCI)

Interested in publishing with us?
Contact book.department@intechopen.com

Numbers displayed above are based on latest data collected.
For more information visit www.intechopen.com

Chapter 15

Single-Molecule Recognition and Dynamics with Pulsed Laser Excitation

Guofeng Zhang, Ruiyun Chen, Yan Gao, Liantuan Xiao and Suotang Jia

Additional information is available at the end of the chapter

http://dx.doi.org/10.5772/48688

1. Introduction

Single-molecule spectroscopy has evolved from a specialized variety of optical spectroscopy into a versatile tool used to address a broad range of questions in physics, chemistry, biology, and materials science. Due to the ultra short time duration, the pulsed laser can be applied widely in the research of single-molecule dynamics. In the chapter, we will discuss the laser pulse application in two aspects of single-molecule detection and spectroscopy: fast recognition of single molecules, and manipulation of interfacial electron transfer dynamics.

The chapter is organized as follows. In the part of fast recognition of single molecules, we will discuss the Mandel's Q-parameter of single-event photon statistics for single-molecule fluorescence, recognition of single molecules using Q parameter, and the influence of signal-to-background ratio and the error estimates for fast recognition of single molecules. In the other part of the chapter, we will discuss the manipulation of interfacial electron transfer dynamics. First, we will introduce the principle of fluorescence lifetime measurement. Next, we will show the experiment results of the single-molecule and the ensemble under the external electric currents. Last, we will present our analysis and discussion for the results.

2. Fast recognition of single molecules

Although people most often think about and model molecule systems in terms of individuals, experimental science has been dominated by measurements that result in ensemble averages. This has traditionally hidden much of the rich variety present at microscopic scales. Although detecting single molecules optically was an old dream, the first convincing detection of a single molecule was achieved in 1989 by Moerner and Kador in an absorption measurement (Moerner et al., 1989). Optical spectroscopy offers a wealth of information on the structure, interaction, and dynamics of molecule species. Soon here after, fluorescence was shown to

provide a much better signal-to-noise ratio, in cryogenic condition (Orrit et al., 1990) as well as at room temperature (Shera et al., 1990; Basché et al., 1992). The microscopy of single molecules at room temperature took off in 1993 with Betzig and Chichester's detection of immobilized molecules on a solid surface by means of excitation with a near-field optical source (Betzig et al., 1993). The scope of the method expanded suddenly when several groups (Nie et al., 1994; Trautman et al., 1994; Funatsu et al., 1995; Dickson, et al., 1996) showed that single molecules could be detected at ambient conditions with a simple confocal microscope. Single-molecule microscopy by fluorescence at room temperature has now become a versatile and general technique, opening investigations of the nanoworld (Orrit, 2002; Bartko et al., 2002). In above experiments it is critical to ascertain that the observed signal actually comes from a single molecule, but not the random mixture of emissions from nearby molecules. Usually low concentration and equivalently small excitation volumes are the most common experimental strategies (Deniz et al., 1999).

Once experimental conditions favoring single-molecule detection are satisfied, a number of criteria have to be met to ascertain that the observed signal actually comes from a single emitter (Michalet et al., 2002 ; Nie et al., 1994). The most common criteria is to detect an antibunching curve by two-time correlation measurements: based on quantum properties of single photon states, the absence of coincidence at zero delay gives clear evidence of single photon emission (Brunel et al., 1999). For several molecules, coincident emission of photons by the different molecules are likely and will result in an autocorrelation function that does not cancel out for zero time-delay.

Although the phenomenon of photon antibunching is demonstrated most clearly by two-time correlation measurements, it is, in principle, also exhibited by the probability P(n) that n photons are emitted (or detected) in a given time interval T. Antibunching implies sub-Poissonian statistics, in the sense that the probability distribution is narrower than a Poisson distribution with the same $\langle n \rangle$ (Mandel, 1979). Traditional photon number counting statistics (Huang et al., 2006) is seriously affected by the blinking in the fluorescence, due to the molecular triplet state. Then single event photon statistics (Huang et al., 2007; Treussart et al., 2002) is suggested to character the single-molecule fluorescence. And based on moment analysis, Mandel's Q-parameter, which is defined in terms of the first two photon count moments, is an attractive alternative to two-time correlation measurements. It is quite robust with respect to molecular triplet state effects (Sanchez-Andres et al., 2005). In this work we suggest a novel approach to distinguish single-molecule system based on single event photon statistics characterization of single-molecule fluorescence. Using Hanbury Brown and Twiss (HBT) configuration (Hanbury Brown et al., 1956), by analyzing and comparing the Mandel parameters of actual single molecule fluorescence and ideal double molecule fluorescence, we present a new criterion based on single event photon statistics measurement.

2.1. Detection system of single-molecule fluorescence

Standard confocal microscopy technique (Michalet & Weiss, 2002) which is the commonly used experimental setup for single-molecule fluorescence detection is summarized in Fig.

1(a) , the emitted light from molecules is focused on a pinhole in order to reject out-of-focus background light and then recollimated onto two single photon counting modules (SPCM) after partition by a 50/50 beamsplitter (BS), which is a standard HBT configuration. For each detected photon, the SPCM would generate a TTL pulse.

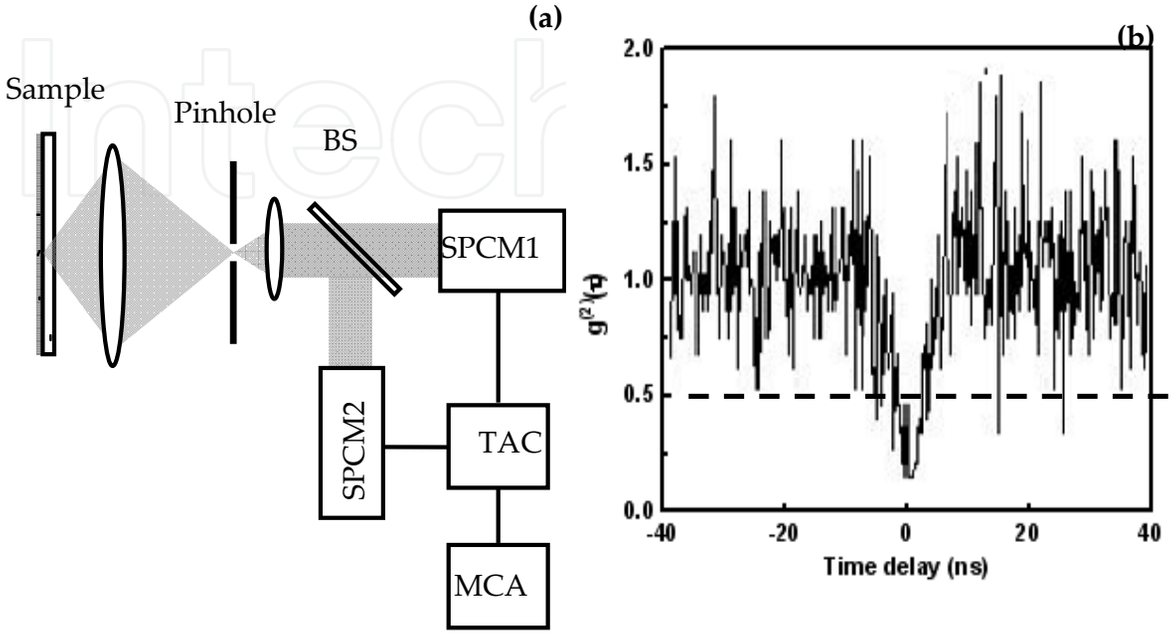

Figure 1. (a) Schematic of a confocal setup used for single-molecule fluorescence detection. (b) The second-order autocorrelation function measured, which indicates that fluorescence of a single molecule was being detected.

2.2. Detection of second-order coherence function

The signals from SPCMs are inputed to a time-to-amplitude converter (TAC). The start-stop technique with allows us to build a coincidences histogram as a function of time delay between two consecutive photodetections on each side of the beamsplitter. Then the pulses from TAC, whose amplitude is proportional to the time delay, are discriminated according to their heights and accumulated by a multichannel pulse height analyzer (MCA). The second-order degree of coherence at zero delay $g^{(2)}(0)$ can be directly gained and displayed on the screen, as shown in Fig. 1(b).

In experiment the effect of background signals makes it impossible for the perfect absence of coincidence at zero delay. Commonly as long as the second-order degree of coherence $g^{(2)}(\tau)$ at zero delay (τ=0) is less than 0.5, which corresponds with two ideal molecules detected, the fluorescence can be considered from a single emitter. Obviously if $g^{(2)}(0)$ is bigger than 0.5, it indicates that the fluorescence detected is emitted from more than one molecule. In contrast, in Fig. 1(b), $g^{(2)}(0)$ is smaller than 0.5, which indicates that one single molecule was being detected. This method is widely used to distinguish single-molecule in experiments. However, for a small number of blinking molecules, the total number of coincident emission might be too low to reject the single-molecule hypothesis with the

antibunching curve. Furthermore the criteria need long time (typically several minutes to tens minutes, depending on the mean photon number $\langle n \rangle$ and the dead-time of detection system) to detect enough photons to accumulate and display a visible antibunching curve. It is severely affected by the molecule's photostability. And the existence of irreversible photobleaching compelled the long time for single molecules recognition to be insufferable in experiments. Using this method, the fluorescent photons detected should be very weak ($\langle n \rangle$ is less than 0.1), otherwise the start-stop technique will bring an error that can not be ignored.

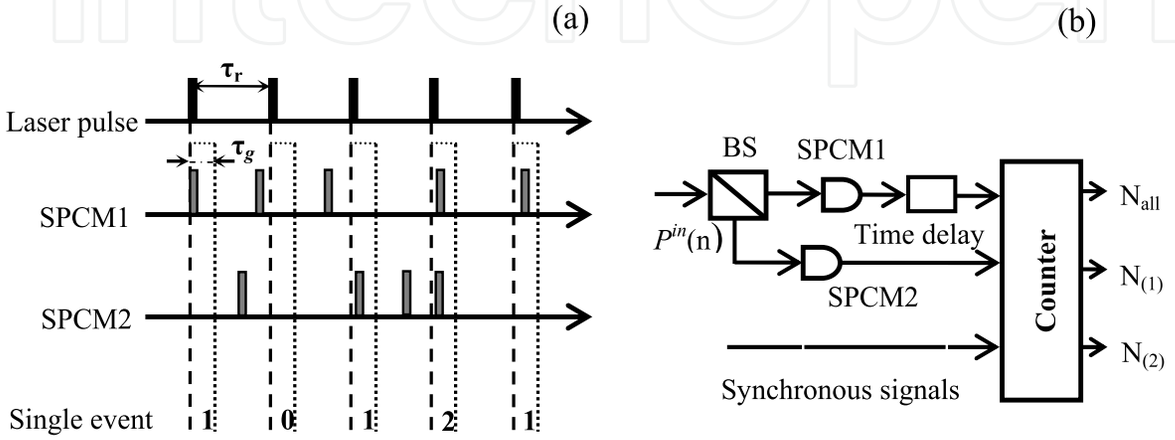

Figure 2. (a) The single event photon statistics measurement. The sample gate time τ_g, dead time for SPCM τ_d and laser pulse period τ_r fulfill $\tau_g<\tau_d<\tau_r$. (b) The schematic of detection setup used for single event photon statistics measurement. The synchronous signals provide a counting time-gate.

2.3. Single event photon statistics characterization of single-molecule fluorescence

The single event photon statistics measurement is described in Fig. 2(a). In order to eliminate the background signals as much as possible, time-gated technique (Shera, et al., 1990) is used after the excitation pulse. The records within the time gates are considered to be the detected signals while all records outside the time gates are rejected. This time-filtering procedure can filter out the real photodetection events from the most of non-synchronous background photocounts not rejected by optical filters, and is often an efficient way to improve the signal-to-noise ratio. The time gate duration must be shorter than the laser period and much longer than the molecule excited-state lifetime so that the probability of discarding a fluorescence signal is negligible. In the above experiments the gate durations are usually ten times the radiative lifetime of the molecule (Alléaume et al., 2004). Furthermore most after-pulse which will show up within 3 ns after the detector dead time, can be eliminated by time-gated technique, when time gate is shorter than the dead time. For the influence of detectors' dead time, each SPCM gives only one count (supposedly with 100% detection efficiency) for one or more than one incident photon within the dead time. For every excitation pulse cycle, the number of detected photons cannot exceed two if we using two identical SPCMs operating in the photon counting regime compulsory for our system. The existence of detectors' dead time in each detection channels will results in a

non-linear relation-ship between detected photon statistics and source photon statistics. Thus the measured photon probabilities should be corrected.

Fig. 2(b) shows the schematic of our detection setup used for single event photon statistics measurement. The synchronous signals provide a counting time-gate and a nanosecond time delay box is used to compensate the different transport distance between two detection channels. The numbers of pulse cycles which are detected N_{all} , in which only one photon is detected $N_{(1)}$, and in which two photons are detected $N_{(2)}$ can be directly gained from a counter. Then the ratio of $N_{(1)}$ to N_{all} and $N_{(2)}$ to N_{all} respectively is the probability of detected one-photon and of detected two-photon in every pulse cycle.

Denoting by $P^{in}(n)$ the photon number probability distribution of incoming light on HBT detection set-up, the non-linear transformation relating this probability to the detected photon probability P(n = 0, 1, 2) is simply calculated for 'ideal' detectors. The 'ideal' means that each SPCM clicks with 100% efficiency immediately upon receiving a photon, but that no more than one click can occur in a given repetition period. The joint probability of detecting i photons on SPCM1 and j photons on SPCM2 can be written as $P(i, j)$, i, j = 0 or 1. Actually, there are total four measured photon probabilities: $P(0, 0)$, $P(0, 1)$, $P(1, 0)$and $P(1, 1)$.

With our experimental detection scheme, random splitting of photons on two sides of 50/50 beamsplitter gives

$$\mathrm{P}(0) = P(0,0) = P^{in}(0),$$

$$\mathrm{P}(1) = P(0,1) + P(1,0) = \sum_{n\geq 1}^{\infty} P^{in}(n)\frac{1}{2^{n-1}}, \tag{1}$$

$$\mathrm{P}(2) = P(1,1) = \sum_{n\geq 2}^{\infty} P^{in}(n)\left(1-\frac{1}{2^{n-1}}\right).$$

The mean photon number per excitation pulse period is

$$\langle n\rangle = \mathrm{P}(1) + 2\mathrm{P}(2). \tag{2}$$

2.4. Mandel's parameter for single event photon statistics

In order to quantify the fluctuations of the number of photons detected per pulse, an important figure of merit is the Mandel parameter $Q = (\langle(\Delta n)^2\rangle - \langle n\rangle)/\langle n\rangle$, where $\langle n\rangle$ is the average number of photons detected within a time interval T and $\langle(\Delta n)^2\rangle$ is the mean variance (Short et al., 1983). The parameter Q is a natural measure of the departure of the variance of the photon number $\langle n\rangle$ from the variance of a Poisson process, for which Q = 0. Negative and positive Q-values indicate sub- and super-Poissonian behavior, respectively.

From single event photon statistics probability the Mandel parameter can be computed directly

$$Q = \frac{2\mathrm{P}(2)}{\langle n \rangle} - \langle n \rangle. \tag{3}$$

Note that an ideal single molecule should produce photons containing exactly one photon per pulse, P(2)=0, would yield $Q_i = -\langle n \rangle = -\eta$, which means Q is only limited by the detection efficiency. Negative Q confirms that single-molecule fluorescence indeed exhibits sub-Poissonian photon statistics which is an explicit feature of a quantum field.

2.5. Distinguishing single-molecule using Q-parameter

The Mandel's Q-parameter provides an alternative for differentiating single-molecule fluorescence system. The Q-parameter of ideal double molecules (which is used to model two molecules that can not be separated by diluting) fluorescence can be used as a boundary between that of an actual single molecule fluorescence and actual double molecules fluorescence. From this boundary we can deduce an explicit criterion of single molecules based on photon statistics.

Now suppose that in the excitation volume there has been more than one molecule, the number is s, and all of them are ideal single photon emitters. We call η the overall detection efficiency, which includes the optical collection efficiency, all linear propagation losses and quantum efficiency of photon detectors. Then the photon number probability distribution of incoming light on detection set-up is

$$P_I^{in}(n) = \frac{s!}{n!(s-n)!}(1-\eta)^{s-n}\eta^n. \tag{4}$$

Applying Eq. (4) in Eq. (1) one can show

$$\mathrm{P}(0) = (1-\eta)^s,$$

$$\mathrm{P}(1) = \sum_{n\geq 1}^{s} \frac{s!}{n!(s-n)!}(1-\eta)^{s-n}\eta^n \frac{1}{2^{n-1}}, \tag{5}$$

$$\mathrm{P}(2) = \sum_{n\geq 2}^{s} \frac{s!}{n!(s-n)!}(1-\eta)^{s-n}\eta^n \left(1-\frac{1}{2^{n-1}}\right).$$

Then

$$\langle n \rangle = s\eta(1-\eta)^{s-1} + \sum_{n\geq 2}^{s} \frac{2^n-1}{2^{n-1}} \frac{s!}{n!(s-n)!}(1-\eta)^{s-n}\eta^n. \tag{6}$$

Now suppose that in the excitation volume there are two ideal molecules excited and the fluorescent photons emitted are detected without background noise at all. Denote by Q_D and $P_D(n)$ the Mandel parameter and single event photon statistics probability of the fluorescence signals. From Eq. (4) one obtains

$$\begin{aligned} \mathrm{P}_D(0) &= (1-\eta)^2, \\ \mathrm{P}_D(1) &= 2\eta - \frac{3}{2}\eta^2, \\ \mathrm{P}_D(2) &= \frac{1}{2}\eta^2, \\ \langle n \rangle &= 2\eta - \frac{1}{2}\eta^2. \end{aligned} \tag{7}$$

In an experiment a problem we have to face is the background signals, which includes radiation from the environment and the dark counts of the SPCM. Because the scattering background light from surroundings can be thought as a thermal field with very large bandwidth and very short coherent time, the usual photon counting time (nano-seconds) discussed here is much longer than the coherent time and the photocounts of such time-average stationary background show a Poisson distribution. In a dark environment, the SPCM also generates random dark counts that follow a Poisson distribution. Both of these two random counts appear in the Poisson distribution, and thus we can use a weak coherent field with a Poisson photon distribution $P_B^{in}(n) = e^{-\eta\gamma}(\eta\gamma)^n / n!$ with γ to simulate the backgrounds. Actual single-molecule fluorescence can be modeled as the superposition of an ideal single molecule and a background emission that can be modeled as a Poisson distribution. Denote by Q_A and $P_A(n)$ the Mandel parameter and single event photon probability statistics of the actual single molecules fluorescence. Using Eq. (1) and Eq. (4), the photon statistics probability can be written as

$$\begin{aligned} \mathrm{P}_A(0) &= e^{-\eta\gamma}(1-\eta), \\ \mathrm{P}_A(1) &= 2\left(e^{-\eta\gamma/2} - e^{-\eta\gamma}\right) + \eta\left(2e^{-\eta\gamma} - e^{-\eta\gamma/2}\right), \\ \mathrm{P}_A(2) &= \left(1 - e^{-\eta\gamma/2}\right)^2 + \eta\left(e^{-\eta\gamma/2} - e^{-\eta\gamma}\right). \end{aligned} \tag{8}$$

Then

$$\langle n \rangle = 2(1 - e^{-\eta\gamma/2}) + \eta e^{-\eta\gamma/2}.$$

The measured mean photon number of fluorescence signals is $S = \eta$, and the measured mean photon number of background signals is $B = 2\left(1 - e^{-\eta\gamma/2}\right)$. According to Eq. (7), we get

$$P_A(0) = (1-S)\left(1-\frac{B}{2}\right)^2,$$

$$P_A(1) = (S+B-SB)\left(1-\frac{B}{2}\right), \tag{9}$$

$$P_A(2) = \frac{BS}{2} + \frac{B^2}{4} - \frac{B^2 S}{4},$$

$$\langle n \rangle = B + S(1-\frac{B}{2}).$$

When

$$P_A(1) \geq 2\sqrt{P_A(2)} - 3P_A(2),$$

the signal-to- background ratio (SBR) can be expressed as

$$SBR = \frac{S}{B} = \frac{P_A{}^2(1)}{2P_A(2)}. \tag{10}$$

This equation can be directly applied for the measurement of SBR in experiment.

Using Eq. (6) one can show that with the same average photon number $\langle n \rangle$, if $P_A(2)<P_D(2)$, then $Q_A<Q_D$. From Eq. (10) one can obtains

$$P_A(2) < \frac{1}{2}\left(2-\sqrt{4-2\langle n \rangle}\right)^2. \tag{11}$$

At the same time,

$$P_A(1) > \langle n \rangle - \left(2-\sqrt{4-2\langle n \rangle}\right)^2. \tag{12}$$

It is not possible to have fluorescence from more than one fluorophore with it's Q-parameter smaller than Q_D. So when Eq. (11) or (12) is satisfied, $Q_A<Q_D$, the fluorescence can be deduced origin from a single molecule system.

2.6. Signal-to-background ratio effect on the criterion

However low background signal is an important precondition of the criterion of Eqs. (11) and (12). With the high background signals, $Q_A > Q_D$ will come into existence for a single molecule system. This criterion will not be applicable. So it is necessary to make certain the range of SBR when Eqs. (11) and (12) is satisfied.

Corresponding to Eqs. (11) and (12) using Eqs. (8) and (9) one can obtains

$$SBR_A > SBR_0 = \frac{\sqrt{\langle n\rangle^2 - 2\left(2-\sqrt{4-2\langle n\rangle}\right)^2}}{\langle n\rangle - \sqrt{\langle n\rangle^2 - 2\left(2-\sqrt{4-2\langle n\rangle}\right)^2} - \frac{1}{2}\left(\langle n\rangle - \sqrt{\langle n\rangle^2 - 2\left(2-\sqrt{4-2\langle n\rangle}\right)^2}\right)^2}. \quad (13)$$

It is well known that SBR of the actual single molecule system varies with average photon number $\langle n\rangle$. Based on Eq. (13), the SBR curve versus $\langle n\rangle$ is shown in Fig. 3. When $\langle n\rangle$ is between 0 and 1, the variation range of SBR is within 1.63 to 2.41. So with the same $\langle n\rangle$ when $SBR_A > SBR_0$, for actual single molecule fluorescence and ideal double molecules fluorescence, it has $Q_A < Q_D$. Especially when SBR > 2.41, the Eqs. (11) and (12) can be the criterion used to distinguish single molecule system. Contrarily when $SBR_A < SBR_0$, even an actual single molecule system can not satisfy the Eqs. (11) and (12). It is obvious that SBR is also an important parameter of distinguishing single molecule system. Nevertheless most of the SBR in single molecule fluorescence experiments is large than 2.41.

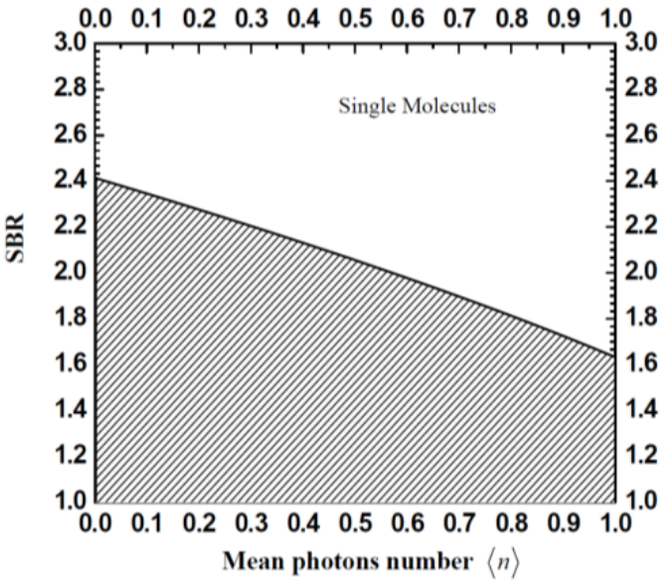

Figure 3. The curve of SBR as a function of the mean photon number $\langle n\rangle$ for actual single molecular photon source. The range out of the shaded portion means the ones that can use the criterion of Eqs. (11) and (12).

2.7. Results and discussion

After error correction from appendix one can obtain a more sufficient criterion,

$$P_A(1) > \langle n\rangle - \left(2-\sqrt{4-2\langle n\rangle}\right)^2 - \delta P_A(1) + \left\langle \Delta P_A(1)\right\rangle = P_1, \quad (14)$$

$$P_A(2) < \frac{1}{2}\left(2-\sqrt{4-2\langle n\rangle}\right)^2 - \delta P_A(2) - \left\langle \Delta P_A(2)\right\rangle = P_2, \quad (15)$$

In the above inequalities the critical values P_1, P_2 are impacted by three parameters, the mean photon number γ of Poissonian background, the mean overall detection efficiency η, and factor Δ which represents the unbalance of two channels of imperfect detection system.

Now let us assume that the size of sample cycles M was 10^4. In this way the statistical fluctuation of the $\langle \Delta P_A \rangle$ induced by finite sample pulse cycles detected can be negligible, which is less than 1/100 of the statistics probability itself. The error δP_A caused by imperfect detection system is the main correction factor of the critical value.

Fig. 4 shows the critical values P_1, P_2 as the function of mean overall detection efficiency η and factor $\Delta = 0.3$, $\gamma = 0.2$, which corresponds to SBR = 5. It is found that the critical values P_1, P_2 all increase with increasing efficiency η as respected, however the P_1 increases slowly while P_2 increases fast. Furthermore because in single molecule experiments $P_A(2)$ is less than $P_A(1)$, the effect of the error on P_2 is more evident than on P_1. So using $P_A(1)$ as the criterion is more feasible.

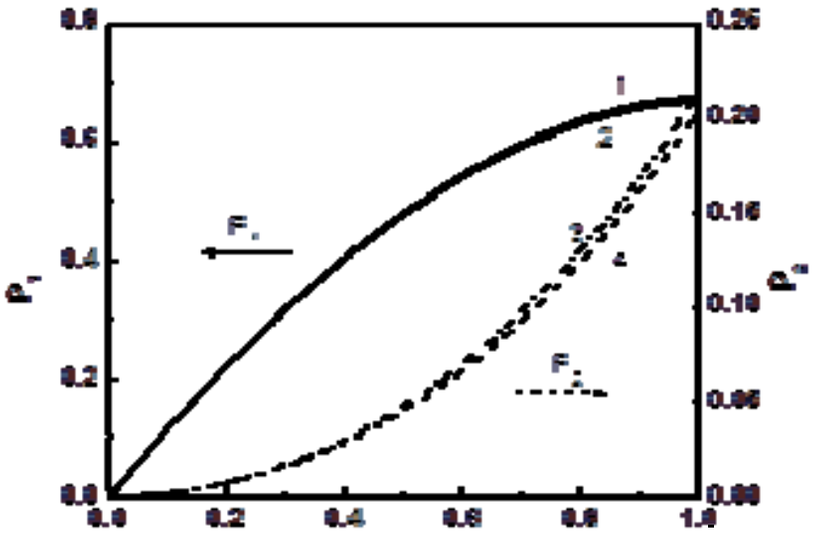

Figure 4. The critical values P_1 (solid line), P_2 (dashed line) as a function of mean overall detection efficiency η. And factor $\Delta = 0.3$, $\gamma = 0.2$, which corresponds to SBR = 5. P_1 (solid line) using left coordinate, P_2 (dashed line) using right coordinate. Curves 2 and 3 are the critical values P_1, P_2 without error estimate. Curves 1 and 4 are the critical values P_1, P_2 after error correction.

The experiment data, shown in Table I, is obtained by using typical single molecule experiment setup (Basché et al., 1992). The sample were dye molecules Cy5 (5×10^{-10} M, Molecular Probes) doped in Polymethyl Methacrylate (PMMA, Sigma-Aldrich) polymer films. Molecules in the sample were excited by 50 ps pulses at a wavelength of 635 nm and repetition rate of 2 MHz, generated by a ps pulsed diode laser (PicoQuant, PDL808), at the focus of a confocal inverted microscope (Nikon). Fluorescence photons were detected in two detection channels, using two identical single photon counting modules (SPCMs, PerkinElmer SPCM-AQR-15).

For example, in a typical experiment to sample 1, during 299613 periods (about 149 ms) there are 13917 recorded photons including 13902 single photon events, 15 two-photons

events. These data allow us to extract the photon probabilities P(0) = 0.9535, P(1) = 0.0464, and P(2) = 5 × 10^{-5} and the mean number of detected photon per pulse $\langle n \rangle$ = 0.0465, then yield Mandel parameter Q = - 0.04435.

We observed fluorescence photons for three sample molecules in one polymer film.

As shown in Table 1, for sample 1 and sample 2, both P(1) are much more than critical values P_1 which indicates that a single molecule was being detected; for sample 3, P(1) is less than critical values P_1 which indicates that more than one molecule was being detected. As a reference, the interrelated results for coherent light (pulse laser) are attached both from theoretical analysis and experimental measurement. The typical time for single event photon statistics measurement is about 150 ms.

	n	P(1)	P_1	$g^{(2)}(0)$	SM?	SBR
Sample 1	0.0465	0.0464	0.04590	0.19	Yes	21
Sample 2	0.0372	0.0370	0.03685	0.30	Yes	7
Sample 3	0.0521	0.0508	0.05150	0.65	No	--
Coherent light (theory)	0.1046	0.0991	0.0991	1.0	--	--
Coherent light (experiment)	0.1046	0.0992	0.0995	0.98	--	--

Table 1. Experimental results of single event photon statistics for Cy5 molecules and coherent light. The mean number $\langle n \rangle$ of detected photons per pulse is calculated by the measured values P(1) and P(2) from Eq. (2). The critical value P_1 is estimated from Eq. (14), the relative error is less than 1%. And the $g^{(2)}(0)$ is measured by two-time correlation measurements. Whether the sample detected is a single molecule is determined by that P(1) is more than critical value P_1 or not. And the determination is confirmed by the measured value $g^{(2)}(0)$. To a single molecule, the SBR is acquired from Eq. (9).

3. Manipulation of interfacial electron transfer dynamics

Interfacial electron transfer (IET) dynamics play an important role in many chemical and biological processes (Weiss, 1676; Wang et al., 2009). However, IET processes are usually very complex due to high dependence on its local environments. Single-molecule spectroscopy has led to many surprises and has now become a standard technique to study complex structures (Kulzer et al., 2010) or dynamics (Orrit et al., 2002; Uji-i et al., 2006; Zhang et al., 2010) including photoinduced, excited-state intramolecular, and IET dynamics. The optical signals of single molecules provide information about dynamics of their nanoscale environment, free from space and time averaging. Single-molecule studies of photoinduced electron transfers in the enzyme flavin reductase have revealed formational fluctuation at multiple time scales (Yang et al., 2003). Single-molecule studies of photosensitized electron transfers on dye containing nanoparticles also showed fluorescence fluctuations and blinking, and the fluctuation dynamics were found to be inhomogeneous from molecule to molecule and from time to time (Funatsu et al., 1995). Recently developed single-molecule spectroelectrochemistry extends single-molecule approaches to ground

state IET by simultaneously modulating the electrochemical potential while detecting single molecule fluorescence (Palacios et al., 2006; Lei et al., 2009).

Indium tin oxide (ITO) films are the most widely used material as a transparent electrode of organic light emitting diode and also in other devices like solar cells (Friend et al., 1999; Tak et al., 2002; Hanson et al., 2005). It is interesting to study electron transfer of ITO to suitably modify interactions at the interfaces of dissimilar materials so that desired electronic properties of devices incorporating them can be realized. Single dye molecules dispersed on the semiconductor surface of ITO were used to measure IET from excited cresyl violet molecules to the conduction band of ITO or energetically accessible surface electronic states under ambient conditions by using a far-field fluorescence microscope, and single-molecule exhibited a single-exponential electron transfer kinetics (Lu et al., 1997). Here we apply an external electric current (EEC) to manipulate the IET rate between single dye molecules and its neighboring ITO nanoparticles by probing the fluorescence intensity change of individually immobilized single dye molecules dispersed in ITO film.

3.1. Experimental section

Cover glass substrates were cleaned by acetone, soap solution, milliQ water sonication and irradiation with ultraviolet lamp. The single molecules samples were prepared by spin coating (3000 rpm) a solution of 1,1′- dioctadecyl - 3, 3, 3′, 3′-tetramethylindodi-carbocyanine (DiD, 10^{-9}M, Molecular Probes) in chlorobenzene onto the cover glass substrate. The chemical structure of DiD molecule is shown in Fig. 5(a). The indium tin oxide (ITO) was purchased from Sigma-Aldrich (Product Number: 700460, dispersion, <100 nm particle size (DLS), 30 wt. % in isopropanol, composition: In_2O_3 90%, SnO_2 10%). ITO film in hundreds of nanometer thicknesses was spin-coated onto the dye molecules. Two aluminum leads were fixed to the ITO film, and the interval between the two leads is about 4 mm. After vacuum-dried, the samples were further covered with a poly-(methyl methacrylate) (PMMA) (Mw = 15,000, Tg = 82 °C, Aldrich) film in order to insulate oxygen. The samples were subsequently annealed in vacuum at 350 K for 5 h to remove residual solvent, oxygen and to relax influences of the spin coating technique on the polymer conformations. The method is depicted schematically in Fig. 5(b).

A 70 picosecond pulse diode laser of λ = 635 nm (PicoQuant, PDL808) with a repetition rate of 40 MHz was used to excite single dye molecules. The output of the pulse laser passed through a polarizing beamsplitter cubes (New Focus 5811) to obtain linear polarization light. A 1/4 wave-plate was used to change the polarized laser into circular polarization light. The laser beam was sent into a conventional inverted fluorescence microscope (Nikon ECLIPSE TE2000-U) from its back side, reflected by a dichroic mirror (BrightLine, Semrock, Di01-R635-25x36), and focused by an oil immersion objective lens (Nikon, 100 ×, 1.3 NA) onto the upper sample surface of the cover glass substrate. The fluorescence was collected by the same objective lens and then passed through the dichroic mirror, an emission filter (BrightLine, Semrock, FF01-642/LP-25-D), and a notch filter (BrightLine, Semrock, NF03-633E-25), is focused onto a 100 μm pinhole for spatial filtering to reject out-of-focus photons.

Fluorescence photons were subsequently focused through a lens and collected by a single-photon detector (PerkinElmer, SPCM-AQR-15). A piezo-scan stage (Piezosystem jena, Tritor 200/20 SG) with an active x-y-z feedback loop mounted on the inversion microscope was used to scan the sample over the focus of the excitation spot, producing a two-dimensional fluorescence imaging. All measurements were conducted in a dark compartment at room temperature. We use an alternative power source to supply EEC for the DID/ITO film system. Here, the applied electric current is proportional to the amplitude of applied external bias voltage, with the relation being I = ZU with Z = 0.87ohm^{-1}. The dye molecules embedded in the ITO film are distinct from the molecules in electric field experiments (Hania et al 2006). In the electric field experiments, a large electric field intensity of about 100 V/μm is needed, and dyes must be insulated from the electrode. In our experiment, dye molecules directly contact with ITO nanoparticles for IET controlling with much low voltage needed (less than 0.02 V/μm). In order to distinguish with the normal electric field experiments, we discuss the results ensuing from EECs here.

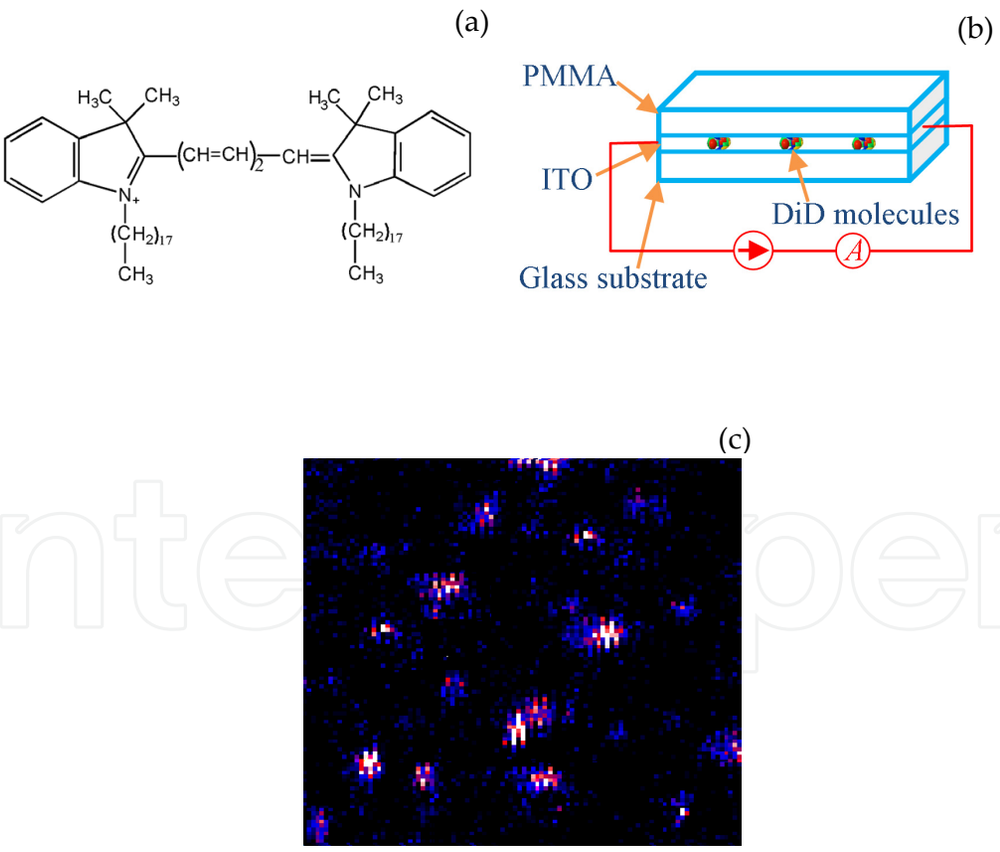

Figure 5. Fig. 5 (a) Structure of the 1, 1′-dioctadecyl-3, 3, 3′, 3′-tetramethylindodicarbocyanine (DiD) dyes molecule. (b) Schematic structure of the sample preparation. (c) Confocally scanned fluorescence image (10 μm × 10 μm) of DiD molecules dispersed in an indium tin oxide (ITO) film. Each bright feature may be attributed to a single DiD molecule.

3.2. Results and discussion

3.2.1. Fluorescence imaging of single dye molecules in ITO film

Fluorescence imaging using a confocal arrangement has superior sensitivity for spectroscopic measurements and is most suitable for studying single-molecule behavior in dilute sample. Fig. 5(c) displays the confocal fluorescence image of the single DiD molecules within a 10 μm × 10 μm area, which is obtained by scanning a sample containing randomly placed isolated single fluorescent molecules dispersed in an ITO film. The imaging is taken in 225 s (150 pixels × 150 pixels), with a pixel integration time of 10 ms. The single molecules are excited with laser excitation intensity of 1.5 kW/cm^2 at 40 MHz. The concentration of the DiD molecules was kept at such a low level that either one molecule or no molecules were in the focus. The bright features in the image then represent the fluorescence from individual molecules. The full width at half maximum of typical spots is about 300 nm. Meanwhile, it is also found that the spots have different intensities due to the molecular orientations and local environments. We have found that the average intensities of the molecules were about an order of magnitude weaker than that of DiD molecules in PMMA without ITO under the same experimental conditions. The weaker signal intensities result from the molecules undergoing the IET with surrounding ITO nanoparticles (Lu, et al., 1997).

3.2.2. Electric current response of the ensemble fluorescence

To study the IET dynamics between dye molecules and ITO nanoparticles, we placed dyes embedded in ITO film. An EEC was added to the DiD/ITO film to manipulate the IET rate. The molecules fluorescence intensity was measured by centering ensemble or one molecule in the laser focus and recording the transient fluorescence intensity, while a time-dependent EEC was applied.

We measured the EEC response of the ensemble at different dyes concentration, and the ensemble averaged study would establish how the average fluorescence intensity and lifetime are affected by the electrical current. The Fig. 6 shows three typical ensemble average results. Fig. 6(a) shows that the fluorescence intensity of an ensemble decreases rapidly while EEC applyed. Fig. 6(b) shows a fluorescence quenching trajectory of an ensemble under the EEC. However, fluorescence can be enhanced sometimes for some ensembles at relative small EECs as shown in Fig. 6(c). The similar fluorescence enhancement was also observed(Palacios et al., 2009), which was explained that potential-induced modulation of the excited state reduction processes (i.e., electron transfer from ITO to the molecules) dominate the low-potential fluorescence-modulation effect. We can find from the Fig. 6 that the ensembles do not show complete fluorescence quenching at the relative large EEC. This may be due to that those dye molecules in the ensemble are not in good contact with the ITO nanoparticles, which shows poor IET.

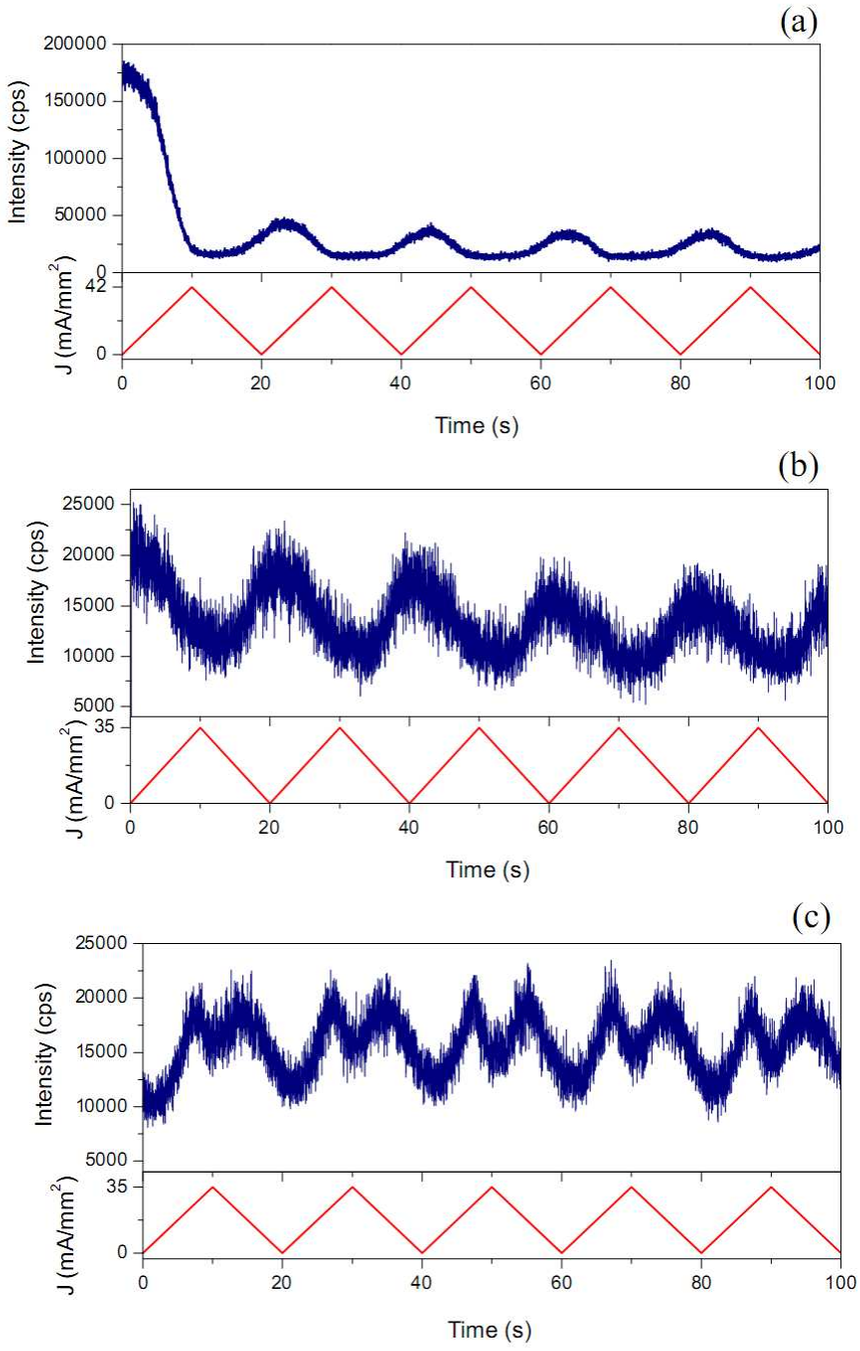

Figure 6. Three typical patterns of ensemble fluorescence intensity trajectories that were obtained while repeatedly applying a triangle wave EEC sequence to ITO shown by the bottom red curves. (a) The fluorescence intensity shows a fast quenching while applying the EEC to the ITO. (b) The fluorescence intensity shows a decrease while applying the EEC to the ITO. (c) The trajectory shows that fluorescence increases at smaller EEC and then decreases at larger EEC.

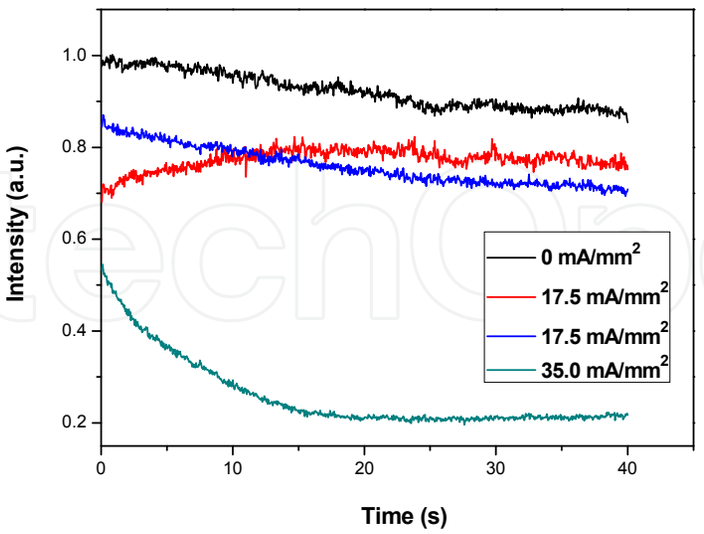

Figure 7. Normalized fluorescence intensity trajectories of 25 ensembles obtained at different EECs. The black curve shows the average of 25 ensemble trajectories obtained at zero current; the blue curve shows the average of 16 ensemble trajectories with fluorescence quenching obtained at the currentF of 17.5 mA/mm^2; the red curve shows the average of 9 ensemble trajectories with fluorescence enhancement obtained at the current density of 17.5 mA/mm^2; the green curve shows the average of 25 ensemble trajectories obtained at the current density of 35.0 mA/mm^2.

Normalized fluorescence intensity trajectories of 25 ensembles with different dyes concentration obtained under different EECs is shown in Fig. 7. Under relative small EECs, some ensembles show fluorescence quenching and the other ensembles show fluorescence enhancement, and the red curve and blue curve are constructed by sorting trajectories with fluorescence enhancement and fluorescence quenching at the current density of 17.5 mA/mm^2. In our experiment, for approximately 30% of the ensemble data show fluorescence enhancement effects at relative small current. The green curve is the average of 25 ensemble trajectories obtained at the current density of 35.0 mA/mm^2, and it shows fluorescence quenching of the ensemble at a large current. The various responses to EECs arise from the heterogeneity of site-specific molecules.

3.2.3. Electric current response of single-molecule fluorescence

We have detected several hundreds of single DiD molecules and all of the molecules sensitively responded to EEC. Fig. 8 shows the typical fluorescence emission for different individual DiD molecules in dependence of the EEC as a function of time. Fig. 8(a) is the fluorescence intensity time trace of one DiD molecule as an EEC of 32.0 mA/mm^2 periodically applied to the ITO film, which shows that the EEC can effectively quench the fluorescence emission of single-molecule. Fluorescence blinking observed in the trace shows a single DiD molecule emission and the blinking is related to the triplet state and/or charge transfer between single molecule and its local environment. While the electric current

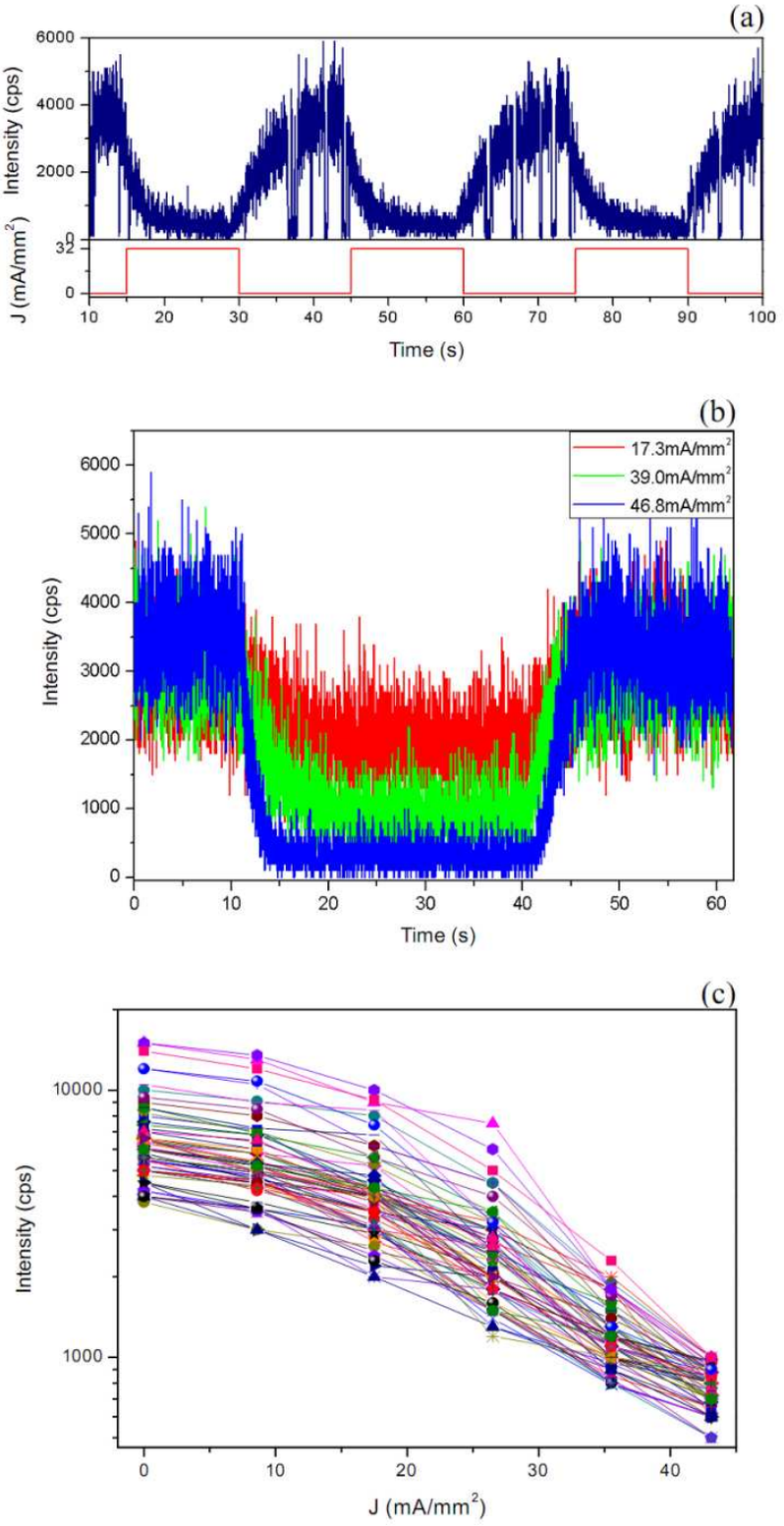

Figure 8. EEC response of DiD single-molecule emission intensity. (a) One single molecule fluorescence emission patterns as electric current applied periodically to the electrodes. (b) Another single-molecule emission intensities under different electric currents applied between 10 s and 40 s. (c) Single-molecule fluorescence intensity trajectories (data points) for 75 DiD single molecules that were obtained while applying different EECs.

density of 32.0 mA/mm² is applied to the electrodes, the fluorescence intensities of the single molecule exhibit an exponential decay with the time constant about 2.24 ± 0.23 s. The fluorescence emission gradually recovers to the initial value which needs about 10 s after switching off the EEC. We find that both of the decay time and the recovering time depend on the molecular neighboring environment. The emission intensities of another single molecule at different electric currents are showed in Fig. 8(b), note that the rates of intensity decay are different, when electric currents are applied between 10 s and 40 s. These intensity decay traces were fitted by single-exponential function with the time constants of 5.80 ± 1.20 s, 3.20 ± 0.54 s and 1.38 ± 0.09 s under the electric current density of 17.3 mA/mm², 39.0 mA/mm², and 46.8 mA/cm² respectively. Note that the bigger current, the faster response. The intensities recover to the initial values which need about 7.5 s after switching off the EEC. It is also found from the Fig. 8(b) that the 46.8 mA/mm² current density (and even bigger) can quench almost completely the fluorescence emission. The two molecules have the different recovering times, which arises from the heterogeneity of site-specific molecular interactions.

In addition, we record the average fluorescence intensities of each single DiD molecule at different currents. The statistical data of 75 DiD single molecules are shown in Fig. 8(c). All the DiD single molecules exhibit intensity decrease with the large EEC.

We present a model, as shown in the Fig. 9, to explain the results of fluorescence quenching of single-molecule. The schematic representation of energy levels, basic photoinduced and electric current driving processes, and multiple electron transfer cycles in DiD / ITO system are shown.

When an EEC is applied to the ITO film, the Fermi level of the ITO is tuned by the potential. With a positive potential, the Fermi level of ITO is decreased and there is more driving force for the forward electric transfer (FET) and the electron transfer of ground state (GET), but backward electron transfer (BET) is suppressed simultaneously.

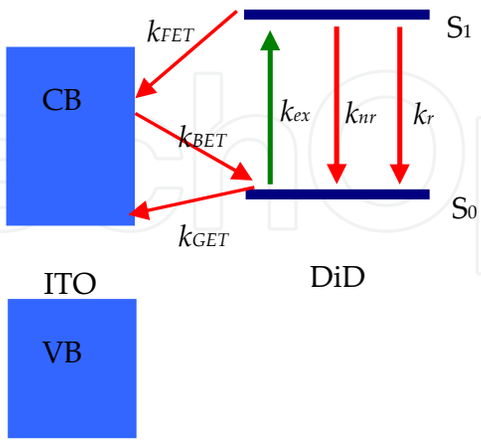

Figure 9. Schematic representation of energy levels, basic photoinduced and electric current driving process, and multiple electron transfer cycles in DiD / ITO system. k_r, radiative decay rate; k_{nr}, intrinsic nonradiative decay rate; k_{FET}, the rate of forward interfacial electron transfer from excited molecule to semiconductor; k_{BET}, the rate of backward electron transfer; k_{GET}, the rate of electron transfer from ground state of molecule to ITO; CB, the conduction band of ITO; VB, the valence band of ITO.

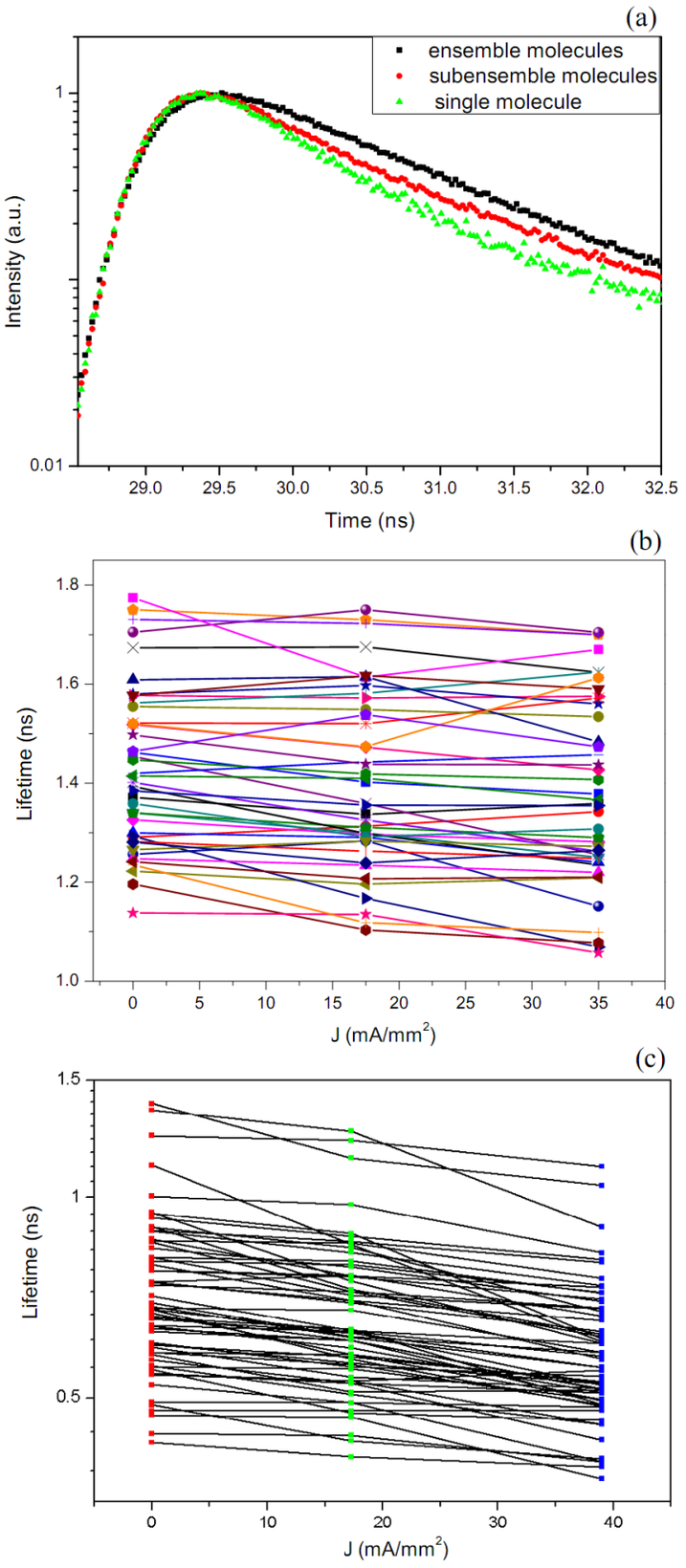

Figure 10. (a) Fluorescence decays for an ensemble molecules (black curve), a subensemble molecules (red curve) and a single molecule (green curve) in ITO film, measured by time correlated photon counting. The decay curves are fitted with single-exponential decay with the time constant about 1.41

ns, 1.16 ns and 0.90 ns respectively. (b) The fluorescence lifetimes of ensemble average for 45 ensembles at three different electric currents. The average fluorescence lifetime is 1.43 ns at 0 mA/mm^2, 1.40 ns at 17.5 mA/mm^2, and 1.38 ns at 35.0 mA/mm^2 respectively. (c) The fluorescence lifetimes of 65 single molecules at three different electric currents. The average fluorescence lifetime is 0.73 ns at 0 mA/mm^2, 0.67 ns at 17.3 mA/mm^2, and 0.59 ns at 39.0 mA/mm^2 respectively.

While the BET is suppressed completely at a large EEC, the fluorescence is completely quenched. When EEC is switched off, the Fermi level of ITO will gradually recover to its original value and the driving force for the FET and GET will decrease, simultaneously the BET will increase, thus the fluorescence will recover gradually.

3.2.4. Electric current dependence of fluorescence lifetime

Lu and Xie have presented that each single molecule exhibits a single-exponential IET dynamics in dye molecules / ITO film system, the rate of FET, k_{FET}, can be measured by the fluorescence decay of excited dye molecules. And the changes of fluorescence lifetimes were attributed to the FET (Guo et al., 2007; Wang et al., 2009; Jin, 2010).

Fig. 10(a) shows three typical fluorescence decay curves for an ensemble (average intensity is about 800 k cps), a subensemble (average intensity is about 40k cps) and a single DiD molecule (average intensity is about 8 k cps) in ITO film. The decay curves are fitted with single-exponential decay with the time constant about 1.41 ns, 1.16 ns and 0.90 ns respectively. Accordingly, the lifetimes of DiD single-molecule are shorter than the 2.5 ns ~ 3.0 ns lifetime measured in the polymer (Vallée et al., 2003). Fig. 10(b) shows that the fluorescence lifetimes of ensemble average for 45 ensembles at three different electric currents, ranging from 1.1 ns to 1.8 ns. The average fluorescence lifetime is 1.43 ns at 0 mA/mm^2, 1.40 ns at 17.5 mA/mm^2, and 1.38 ns at 35.0 mA/mm^2 respectively. Fig. 10(c) shows fluorescence lifetimes of 65 DiD single molecules at three different electric currents, ranging from ~300 ps to 1.4 ns. The average fluorescence lifetime is 0.73 ns at 0 mA/mm^2, 0.67 ns at 17.3 mA/mm^2, and 0.59 ns at 39.0 mA/mm^2 respectively. Unfortunately, we cannot measure a single-molecule lifetime shorter than 300 ps due to the limited sensitivity for time resolution of the instrumental response. As mentioned above, the FET rate is highly sensitive to the interactions between the dyes and ITO nanoparticles. When some dye molecules in the ensemble that are not in good contact with the ITO nanoparticles there will induce the poor IET dynamics. Thus, fluorescence lifetime of the ensemble is longer than the lifetime of single-molecule. In the typical dye-photosensitization system, FET can shorten the fluorescence lifetime and reduce fluorescence quantum yield of the dye molecules. Under the EEC, the small change of fluorescence lifetimes may indicate the change of the FET rate, and the fluorescence quenching may be mainly dominated by the BET and GET.

4. Conclusion

We present a fast and robust method to recognise single molecules based on single event photon statistics. Mandel's Q-parameter provides an attractive approach to two-time

correlation measurements, because it is easy to implement, requires little time, and is immune with respect to the effects of molecular triplet state. Compared with common two-time correlation measurements, our approach has some advantages: (1) the effect of molecular triplet state can be ignored, whereas its effect can only be contained in the non-perfect detection efficiency analysis; (2) ~ ms level measurement time is needed as only ~10^4 fluorescence photons are needed for photon statistic; (3) it is not limited only to weak photons emitted, which means it is independent with the fluorophores photon intensity. The method can also be applied for the other single emitters recognition, such as single atoms, quantum dots and color centers.

Individual DiD dye molecules were dispersed in ITO semiconductor films as probes of IET dynamics, which should help to understand the intrinsic properties of electron transfer at interface between organic molecules and transparent semiconductor materials. While the EEC was used to drive the FET and GET, and suppress the BET, the change of k_{FET} induces the change of fluorescence lifetime and the increasing k_{GET} and decreasing k_{BET} would quench the fluorescence. Due to the inhomogeneous nature of the interactions from molecule to molecule, the lifetime under EEC is inhomogeneous. The EEC dependence of lifetime distribution clearly demonstrates a manipulated IET dynamics, which can be revealed by the single-molecule experiments instead of by the ensemble-averaged measurements. The results could open up a new path to manipulate single-molecule electron transfer dynamics by using EEC while measuring single-molecule fluorescence intensity and lifetime simultaneously.

Author details

Guofeng Zhang, Ruiyun Chen, Yan Gao, Liantuan Xiao and Suotang Jia
State Key Laboratory of Quantum Optics and Quantum Optics Devices,
Laser Spectroscopy Laboratory, Shanxi University, Taiyuan, China

Acknowledgement

The project sponsored by 973 Program (Nos. 2012CB921603, 2010CB923103), 863program (No. 2011AA010801),the Natural Science Foundation of China (Nos. 11174187，11184145, 60978018 and 10934004), NSFC Project for Excellent Research Team (No. 61121064), the Natural Science Foundation of Shanxi province, China (No. 2011091016), TSTIT and TYMIT of Shanxi, and Shanxi Province Foundation for Returned scholars.

5. References

Alléaume, R.; Treussart, F.; Courty, J. M. & Roch, J. F. (2004). Experimental open-air quantum key distribution with a single-photon source, *New J. Phys.*, Vol. 6, No. 92, (March 2004) page number (1-12), ISSN: 1367-2630

Bartko, A. P.; Xu, K. & Dickson, R. M. (2002). Three-dimensional single molecule rotational diffusion in glassy state polymer films, *Phys. Rev. Lett.*, Vol. 89, No. 2, (July 2001) page numbers (026101-1-4), ISSN: 0031-9007

Basché, T. & Moerner, W. E. (1992). Energetics of negatively curved graphitic carbon, *Nature*, Vol. 355, No. 6358, (January 1992) page numbers (333-335), ISSN: 0028-0836

Betzig, E. & Chichester, R. J. (1993). Single molecules observed by near-field scanning optical microscopy, *Science*, Vol. 262, No. 5138, (September 1993) page number (1422-1425), ISSN: 0036-8075

Brunel, C.; Lounis, B.; Tamarat P. & Orrit, M. (1999). Triggered source of single photons based on controlled single molecule fluorescence, *Phys. Rev. Lett.*, Vol. 83, No. 14, (February 1999) page numbers (2722-2725), ISSN: 0031-9007

Deniz, A. A.; Dahan, M.; Grunwell, J. R.; Ha, T.; Faulhaber, A. E.; Chemla, D. S.; Weiss, S. & Schultz, P. G. (1999). Single-pair fluorescence resonance energy transfer on freely diffusing molecules: Observation of Förster distance dependence and subpopulations, *Proc. Nat. Acad. Sci.USA,* Vol. 96, (March 1999) page number (3670-3675), ISSN: 0027-8424

Dickson, R. M.; Norris, D. J.; Tzeng, Y. L. & Moerner, W. E. (1996). Three-dimensional imaging of single molecules solvated in pores of poly(acrylamide) gels, *Science*, Vol. 274, No. 5289, (November 1996) page number (966-968), ISSN: 0036-8075

Friend, R. H.; Gymer, R. W.; Holmes, A. B.; Burroughes, J. H.; Marks, R. N.; Taliani, C.; Bradely, D. D. C.; Dos Santos, D. A.; Bredas, J. L.; Logdlund, M. & Salaneck, W. R. (1999). Electroluminescence in conjugated polymers, *Nature,* Vol. 397, (January 1999) page numbers (121-128), ISSN: 0028-0836

Funatsu, T.; Harada, Y.; Tokunaga, M.; Saito, K. & Yanagida, T. (1995). Imaging of single fluorescent molecules and individual ATP turnovers by single myosin molecules in aqueous solution, *Nature*, Vol. 374, (April 1995) page numbers (555-559), ISSN: 0028-0836

Guo, L.; Wang, Y. & Lu, P. H. (2010). Combined single-molecule photon-stamping spectroscopy and femtosecond transient absorption spectroscopy studies of interfacial electron transfer dynamics, *J. Am. Chem. Soc.,* Vol. 132, No. 6, (January 2010) page numbers (1999-2004), ISSN: 0002-7863

Hanbury, B. R. & Twiss, R. Q. (1956). Correlation between photons in two coherent beams of light, *Nature*, Vol. 177, (January 1956) page numbers (27-29), ISSN: 0028-0836

Hania, P. R., Thomsson, D. & Scheblykin, I. G. (2006). Host matrix dependent fluorescence intensity modulation by an electric field in single conjugated polymer chains, *J. Phys. Chem. B*, Vol. 110, No. 51, (December 2006) page numbers (25895-25900), ISSN: 1520-6106

Hanson, E. L.; Guo, J.; Koch, N.; Schwartz, J. & Bernasek, S. L. (2005). Advanced surface modification of indium tin oxide for improved charge injection in organic devices, *J. Am. Chem. Soc.,* Vol. 127, No. 28, (June 2005) page numbers (10058-10062), ISSN: 0002-7863

Huang, T.; Dong, S. L.; Guo, X. j.; Xiao, L. T. & Jia, S. T. (2006). Signal-to-noise ratio improvement of photon counting using wavelength modulation spectroscopy, *Appl.*

Phys. Lett., Vol. 89, No. 6, (November 2005) page number (061102-061102-3), ISSN: 0003-6951

Huang, T.; Wang, X. B.; Shao, J. H.; Guo, X. J.; Xiao, L. T. & Jia, S. T. (2007). Single event photon statistics characterization of a single photon source in an imperfect detection system, *J. Lumin.*, Vol. 124, No. 2 (August 2005) page number (286-290), ISSN: 0022-2313

Jin, S.; Snoeberger III, R. C.; Issac, A.; Stockwell, D.; Batista, V. S. & Lian, T. (2010). Single-molecule interfacial electron transfer in donor-bridge-nanoparticle acceptor complexes, *J. Phys. Chem. B,* Vol. 114, No. 45, (March 2010) page numbers (14309-14319), ISSN: 1520-6106

Kulzer, F.; Xia, T. & Orrit, M. (2010). Single molecules as optical nanoprobes for soft and complex matter, *Angew. Chem. Int. Ed.,* Vol. 49, No. 5, (January 2010) page numbers (854-866), ISSN: 1433-7851

Lei, C. H.; Hu, D. H. & Ackerman, E. (2009). Clay nanoparticle supported single-molecule fluorescence spectroelectrochemistry, *Nano Lett.,* Vol. 9, No. 2, (January 2009) page numbers (655-658), ISSN: 1530-6954

Lu, H. P. & Xie, X. S. (1997). Single-molecule kinetics of interfacial electron transfer, *J. Phys. Chem. B,* Vol. 101, No. 15, (February 1997) page numbers (2753-2757), ISSN: 1520-6106

Mandel, L. (1979). Sub-poissonian photon statistics in resonance fluorescence, *Opt. Lett.*, Vol. 4, No. 7, (March 1979) page number (205-207), ISSN: 0146-9592

Michalet, X. & Weiss, S. (2002). Single-molecule spectroscopy and microscopy, *C. R. Physique*, Vol. 3, No. 5, (March 2002) page number(619-644), ISSN: 1631-0705

Moerner, W. E. & Kador, L. (1989). Optical detection and spectroscopy of single molecules in a solid, *Phys. Rev. Lett.*, Vol. 62, No. 21, (March 1989) page numbers (2535-2538), ISSN: 0031-9007

Nie, S.; Chiu, D. T. & Zare, R. N. (1994). Probing individual molecules with confocal fluorescence microscopy, *Science*, Vol. 266, No. 5187, (November 1994) page number (1018-1021), ISSN: 0036-8075

Orrit, M. (2002). Single-molecule spectroscopy: The road ahead, *J. Chem. Phys.*, Vol. 119, No. 24, (December 2002) page numbers (10938-10946), ISSN: 0021-9606

Orrit, M. & Bernard, J. (1990). Single pentacene molecules detected by fluorescence excitation in a p-terphenyl crystal. *Phys. Rev. Lett.*, Vol. 65, No. 21, (July 1990) page numbers (2716-2719), ISSN: 0031-9007

Palacios, R. E.; Fan, F. R. F.; Bard, A. J. & Barbara, P. F. (2006). Single-molecule spectroelectrochemistry, *J. Am. Chem. Soc.,* Vol. 128, No. 28, (June 2006) page numbers (9028-9029), ISSN: 0002-7863

Palacios, R. E.; Chang, W. S.; Grey, J. K.; Chang, Y. L.; Miller, W. L.; Lu, C. Y.; Henkelman, G.; Zepeda, D.; Ferraris, J. & Barbara, P. F. (2009). Detailed single-molecule spectroelectrochemical studies of the oxidation of conjugated polymers, *J. Phys. Chem. B,* Vol. 113, No. 44, (October 2009) page numbers (14619-14628), ISSN: 1520-6106

Sanchez-Andres, A.; Chen, Y. & Müller, J. D. (2005). Molecular brightness determined from a generalized form of mandel's Q-parameter, *Biophys. J.*, Vol. 89, No. 5, (May 2005) page number (3531-3547), ISSN: 0006-3495

Shera, E. B.; Seizinger, N. K.; Davis L. M.; Keller, R. A. & Soper, S. A. (1990). Detection of single fluorescent molecules, *Chem. Phys. Lett*., Vol. 174, No.6, (July 1990) page numbers (553-557), ISSN: 0009-2614

Short, R. & Mandel, L. (1983). Observation of sub-poissonian photon statistics, *Phys. Rev. Lett.*, Vol. 51, No. 5, (April 1983) page numbers (384-387), ISSN: 0031-9007

Tak, Y. H.; Kim, K. B.; Park, H. G.; Lee, K. H. & Lee, J. R. (2002). Criteria for ITO (indium–tin-oxide) thin film as the bottom electrode of an organic light emitting diode, *Thin Solid Films,* Vol. 411, No. 1, (May 2002) page numbers (12-16), ISSN: 0040-6090

Trautman, J. K.; Macklin, J. J.; Brus, L. E. & Betzig, E. (1994). Imaging and time-resolved spectroscopy of single molecules at an interface, *Science*, Vol. 272, No. 5259, (April 1996) page number (255-258), ISSN: 0036-8075

Treussart, F. ; Alléaume, R. ; Le Floc'h, V., Xiao, L. T.; Courty, J. M. ; & Roch, J. F. (2002). Direct measurement of the photon statistics of a triggered single photon source, *Phys. Rev. Lett.*, Vol. 89, No. 9, (February 2002) page numbers (093601-1-4), ISSN: 0031-9007

Uji-i, H.; Melnikov, S. M.; Deres, A.; Bergamini, G.; De Schryver, F.; Herrmann, A.; Müllen, K.; Enderlein, J. & Hofkens, J. (2006). Visualizing spatial and temporal heterogeneity of single molecule rotational diffusion in a glassy polymer by defocused wide-field imaging, *Polymer,* Vol. 47, No.7, (March 2006) page numbers (2511-2518), ISSN: 0032-3861

Vallée, R. A. L.; Tomczak, N.; Kuipers, L.; Vancso, G. J. & van Hulst, N. F. (2003). Single molecule lifetime fluctuations reveal segmental dynamics in polymers, *Phys. Rev. Lett.*, Vol. 91, No. 3, (July 2003) page numbers (1038301-1--1038301-4), ISSN: 0031-9007

Wang, Y. M.; Wang, X. F.; Ghosh, S. K. & Lu, H. P. (2009). Probing single-molecule interfacial electron transfer dynamics of porphyrin on TiO2 nanoparticles. *J. Am. Chem. Soc.,* Vol. 131, No. 4, (January 2009) page numbers (1479-1487), ISSN: 0002-7863

Wang, Y. M.; Wang, X. F. & Lu, H. P. (2009). Probing single-molecule interfacial geminate electron−cation recombination dynamics, *J. Am. Chem. Soc.,* Vol. 131, No. 25, (June 2009) page numbers (9020-9025), ISSN: 0002-7863

Weiss, S. (1999). Fluorescence spectroscopy of single biomolecules, *Science,* Vol. 283, No. 5408, (March 1999) page numbers (1676-1683), ISSN: 0036-8075

Yang, H.; Luo, G. B.; Karnchanaphanurach, P.; Louie, T. M.; Rech, I.; Cova, S.; Xun, L. Y. & Xie, X. S. (2003). Protein conformational dynamics probed by single-molecule electron transfer, *Science,* Vol. 302, No. 5643, (October 2003) page numbers (262-266), ISSN: 0036-8075

Zhang, G. F.; Xiao, L. T.; Zhang, F.; Wang, X. B. & Jia, S. T. (2010). Single molecules reorientation reveals the dynamics of polymer glasses surface, *Phys. Chem. Chem. Phys.*, Vol. 12, (December 2009) page numbers (2308-2312), ISSN: 1463-9076